CHARACTERIZATION OF HIGH ENERGY IRRADIATED MOS STRUCTURES USING THE CAPACITANCE METHODS

P. Písečný, Ľ. Stuchlíková, L. Harmatha, M. Ťapajna, O. Csabay

Department of Microelectronics, Faculty of Electrical Engineering and Information Technology, Slovak University of Technology, Ilkovičova 3, 812 19 Bratislava, Slovakia
fax: ++421-2-654 23480 - e-mail: pavol.pisecny@stuba.sk

Summary The formation and annealing of radiation-induced defects in MOS structures exposed to 710 MeV Bi ions and 305 MeV Kr ions radiation with a fluency of 10^9 and 10^{10}cm^{-2} have been studied by capacitance methods. Electrical activity of the defects has brought increase of interface trap density D_{it} and a sharp decrease in the generation parameters t_r and τ_g. The parameters of nine deep levels were detected in the investigation MOS structures. Eight of these levels were radiation defects.

1. INTRODUCTION

The influence of irradiation on semiconductor materials and devices is presented in many issues [1-5]. At the same time are resolved the questions of electronic devices radiation hardness, the understanding of a radiation defect creation and its kinetics and an application high energy heavy ion irradiation for a deep implantation.

The scope of this paper is to present the effect of 305 MeV Kr and 710 MeV Bi ions irradiation with a fluency of 10^9cm^{-2} and 10^{10}cm^{-2} on the MOS structures and the behavior of ionizing radiation induced defect on the same structures under an isochronal annealing.

2. EXPERIMENTAL

<100> -oriented *n*-type antimony doped silicon homogeneous wafers with a resistivity of 2-5 Ωcm and a 300 μm thickness were used as a substrate of the investigated MOS structures. The gate SiO_2 layers were prepared by a thermal oxidation in an atmosphere of a dry oxygen at 1050°C for 90 minutes. The thickness of the SiO_2 layer was about 100 nm. All gates were prepared by a vapour deposition of Al (a thickness 1,3 μm) and patterned photo lithographically. After the MOS structures manufacturing the sample was annealed in $N_2 + H_2$ at 460°C for 20 minutes. The ohmic contact from the backside of the wafer was prepared by an Al vapour deposition. These structures were marked D0.

Afterwards, the MOS structures were exposed to a 305 MeV Kr ion irradiation with a fluency of 10^9cm^{-2} (samples D1) and fluency 10^{10}cm^{-2} (D2) and to a 710 MeV Bi ion irradiation with fluency 10^9cm^{-2} (D8) and with a fluency of 10^{10} cm^{-2} (D6) at the Joint Institute for Nuclear Research in Dubna, Russia [6]. Kr and Bi ions distributions in MOS structures after ion exposition calculated by implanted process simulations in the Monte Carlo code, Transport of Ions in Matter (*TRIM-2000*) [7] are shown in Fig. 1. These simulations affirmed the assumptions: the concentration N_{ion} maximum is deep in substrate below the structure active region and its position is greater about 14% after the irradiation by high-energy Bi than Kr ions at the same fluency.

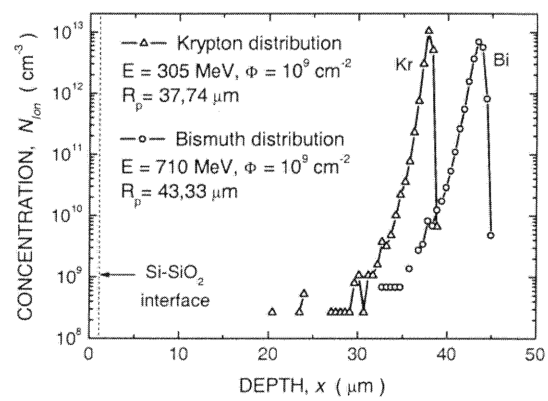

Fig. 1. Krypton and Bismuth ions distribution in MOS structures after ions exposition calculated by simulation program TRIM

On samples D1, D2, D6 an isochronal annealing was carried out for 30 minutes at temperatures 100, 200, 300°C and on sample D8 an isochronal annealing was carried out for 30 minutes at temperatures 150, 300°C.

The non-irradiated MOS structure D0 and the irradiated MOS structures (D1, D2, D6 and D8) were investigated by capacitance methods. The measurements were carried out using an automated set-up designed in our laboratory SEMITEST [8].

Energy distributions of interface trap density of all structures have been determined from the low frequency C-V curve measurement by a quasistatic method. For a low frequency C-V curve measurement was utilized a computer controlled capacitance meter Keithley 595, which implements the charge-voltage method [9].

For the energy distribution determination of the interface trap density it was necessary to know the dependence of band bending on the gate bias

$$\varphi_S = f(U_G) \cdot \qquad (1)$$

This dependence was obtained from integration of the low frequency C-V curve and is given as [10]

$$\varphi_S = \int_{U_{FB}}^{U_G} \left(1 - \frac{C(U_G)}{C_I}\right) dU_G \cdot \qquad (2)$$

The φ_S is linearly proportional to the energy in the band gap

$$E - E_i = q(\varphi_S - \varphi_F)\,. \qquad (3)$$

The capacitance of the interface trap is given as [11]

$$C_{it} = \left(\frac{1}{C_{LF\ real}} - \frac{1}{C_I}\right)^{-1} - \left(\frac{1}{C_{LF\ ideal}} - \frac{1}{C_I}\right)^{-1}, \qquad (4)$$

where $C_{LF\ \mathrm{real}}$ is the measured capacitance and $C_{LF\,\mathrm{ideal}}$ is the ideal capacitance. The density of interface traps is given by [11]

$$D_{it} = \frac{1}{q^2} C_{it}\,. \qquad (5)$$

The flat-band voltage U_{FB} and the free carriers concentration profile $n(x)$ have been determined by a high frequency capacitance-voltage (C-V) method [12].

The relaxation time t_r, generation lifetime of minority charge carriers τ_g and surface generation velocity S_g characterizing the electrical behaviour of defects in the MOS structure have been diagnosed by non-equilibrium C-t method [13].

A depth profile of a generation lifetime $\tau_g(x)$ has been established by a time-domain constant capacitance (cC-t) technique [14]. Multistep cC-t technique is an excellent alternative to the Zerbst technique. Capacitance of an initially deep-depleted MOS-C is maintained at a constant value by increasing the gate charge by a computer-controlled voltage source. The value of generation lifetime is then calculated from the slope of voltage transient, moreover depth profile of the generation lifetime can be obtained.

C-V, C-t and cC-t measurements were performed using the 4280 1 MHz C Meter/C-V Plotter Hewlett-Packard.

Electrically active radiation-induced defects have been studied by standard Deep Level Transient Spectroscopy (DLTS) measurements [15]. DLTS is a high-frequency transient capacitance thermal scanning method, where an electrical excitation pulse causes the capacitance transient effect in a potential barrier of a semiconductor. DLTS measurements have been performed using a Polaron BioRad DLTS spectrometer with a boxcar detection system for acquiring the DLTS output signal. The values of the activation enthalpies ΔE_n of electron deep levels were determined from an Arrhenius diagram using known equations

$$\ln\left(\frac{e_n}{T^2}\right) = \ln(\sigma_n K_n) - \left(\frac{\Delta E_T}{k_B T}\right), \qquad (6)$$

where e_n is the emission rate, K_n - a material constant, T - the absolute temperature, k_B - the Boltzmann constant.

C-V, C-t and standard *DLTS* methods were applied on all irradiated MOS structures before and after the isochronal annealing.

3. EXPERIMENTAL RESULTS AND DISCUSSION

The radiation changes interface trap density D_{it} have been observed at the slope of low frequency C-V curves (Fig. 2) in depletion and weak inversion region and in an increased flat band voltage U_{FB}. We assumed that the increased flat band voltage U_{FB} (Fig. 2 and Fig. 3) is resulted of a rise in the positive defect charge in the oxide and at the interface with the silicon substrate after the high energy heavy Kr an Bi ions irradiation on the MOS structure.

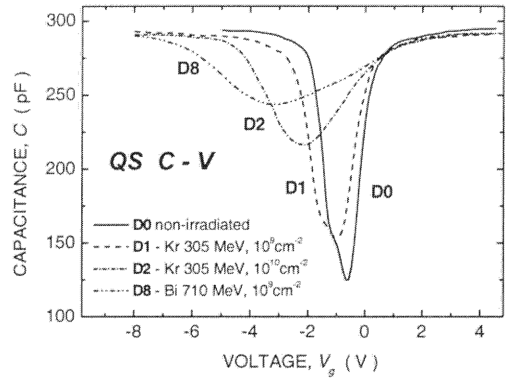

Fig. 2. Low-frequency C-V curves of structures D0, D1, D2, D8

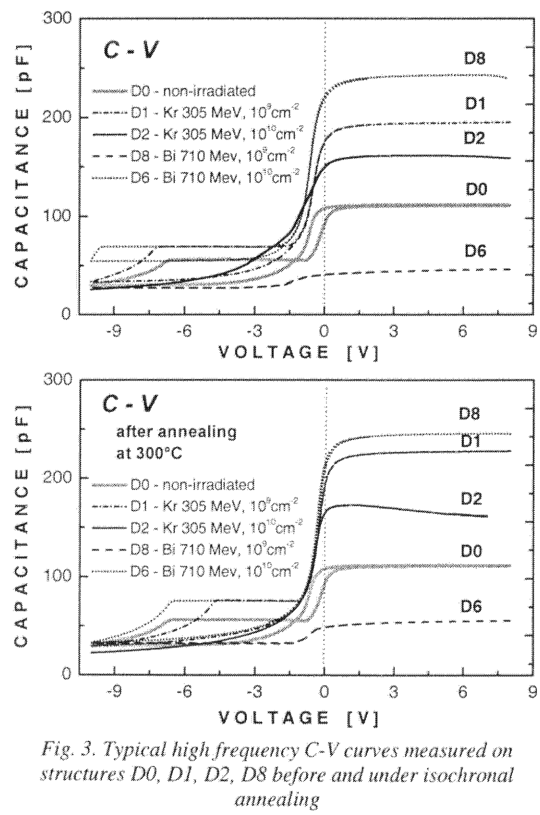

Fig. 3. Typical high frequency C-V curves measured on structures D0, D1, D2, D8 before and under isochronal annealing

The values of D_{it} in Tab.1 were determined at 0,22 eV over the mid-gap (Fig. 4). The non-irradiated sample D0 has the lower value of D_{it}. The D_{it} increasing was observed on the Kr^+ ions irradiated sample D1 (Tab.1). The higher value of

D_{it} in comparison with the sample D1 detected on sample D2 was due to the same radiation with higher fluency. The highest value of D_{it} was observed on the sample D8 irradiated by Bi^+ ions.

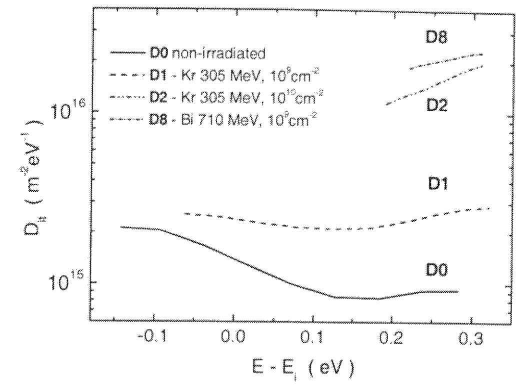

Fig. 4. Energy distribution of interface trap density of structures D0, D1, D2 and D8.

By comparison with the values of the generation surface velocity S_g (Tab.1) obtained from C-t measurements (Fig. 5) we registered a good agreement with the results gained from quasistatic method (D_{it}). Moreover we determined the magnitude of the capture cross-section σ_n, which defines the electrical activity of traps [16]

$$S_g = \sigma_n v_t D_{it}, \qquad (7)$$

where $v_t = 1\cdot10^5\ \mathrm{ms^{-1}}$ is electron thermal velocity for silicon.

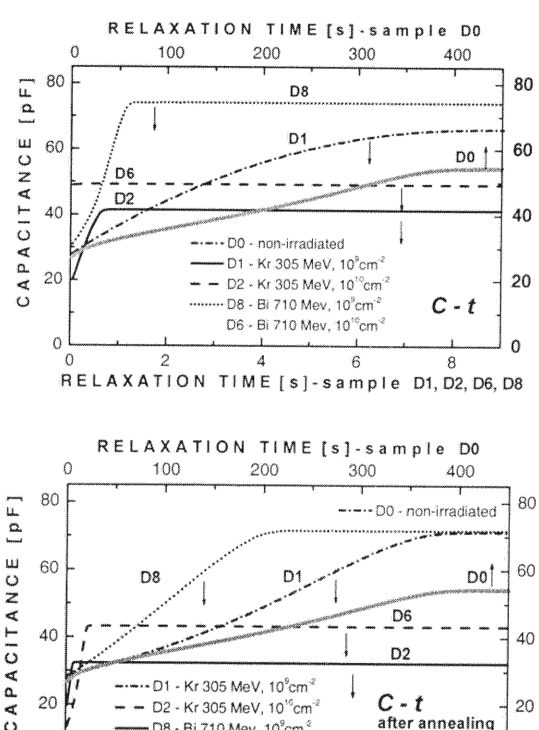

Fig. 5. Typical high frequency C-t curves measured on structures D0, D1, D2, D8 before and under isochronal annealing.

Further from characteristic high frequency C-V (Fig. 3) and C-t (Fig. 5) curves measured on the non-irradiated MOS structures D0 and the irradiated MOS structures D1, before and after annealing we can see that the antimony doped MOS structures had the same or only a slightly lower concentration of impurities N_D. The rise in the density of radiation defects is expressed quantitatively through a considerable decrease of generation lifetime τ_g values and an increase of a generation surface velocity S_g. After the annealing we observed the lengthening of the relaxation time t_r. Annealing temperature increase reveals a reduction of defects and decrease in their activity. Also the changes in τ_g and S_g reveal significant reduction of electrically active defects in the depleted region and on a Si-SiO_2 interface (Tab. 1). Fig. 6 shows a depth profile of a generation lifetime $\tau_g(x)$ on MOS structure D1 after annealing at 300°C obtained by cC-t method. Measured values are in good agreement with result obtained by C-t method. According to

$$1/\tau_g \sim N_T, \qquad (8)$$

where N_T is the trap concentration, we shall assume homogeneous depth distribution of traps in space charge region.

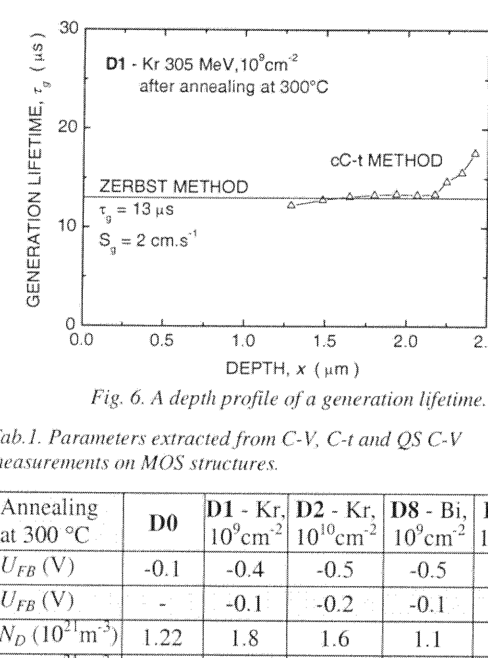

Fig. 6. A depth profile of a generation lifetime.

Tab.1. Parameters extracted from C-V, C-t and QS C-V measurements on MOS structures.

Annealing at 300 °C	**D0**	**D1** - Kr, 10^9cm^{-2}	**D2** - Kr, 10^{10}cm^{-2}	**D8** - Bi, 10^9cm^{-2}	**D6** -Bi 10^{10}cm
U_{FB} (V)	-0.1	-0.4	-0.5	-0.5	-1.2
U_{FB} (V)	-	-0.1	-0.2	-0.1	-0.4
N_D (10^{21}m^{-3})	1.22	1.8	1.6	1.1	0,8
N_D (10^{21}m^{-3})	-	1.8	1.6	1.1	0.8
t_r (s)	487	7.7	0.6	1.7	-
t_r (s)	-	15.2	0.8	8.3	0.46
τ_g (μs)	472	3.9	0.5	1.3	-
τ_g (μs)	-	8.4	0.7	3.5	-
S_g (10^{-2}ms^{-1})	0.22	0.31	13	45	-
S_g (10^{-2}ms^{-1})	-	1.415	2.245	1.16	-
D_{it} (m^{-2}eV^{-1})	$1{,}4\cdot10^{15}$	$2{,}4\cdot10^{15}$	$1{,}3\cdot10^{16}$	$1{,}9\cdot10^{16}$	-
σ_n (10^{-23}m^2)	2,42	1,29	10	24,2·10	

The non-irradiated MOS structures (D0) were of a high quality, having a low density of defects. We detected only one deep energy level DL1 (0,61eV) with a very low concentration $2{\cdot}10^{13}cm^{-3}$ by DLTS measurements. This deep level corresponds to a presence of Au (0,59 eV). Fig. 7 shows typical DLTS spectra measured on the irradiated MOS structures before and after the isochronal annealing.

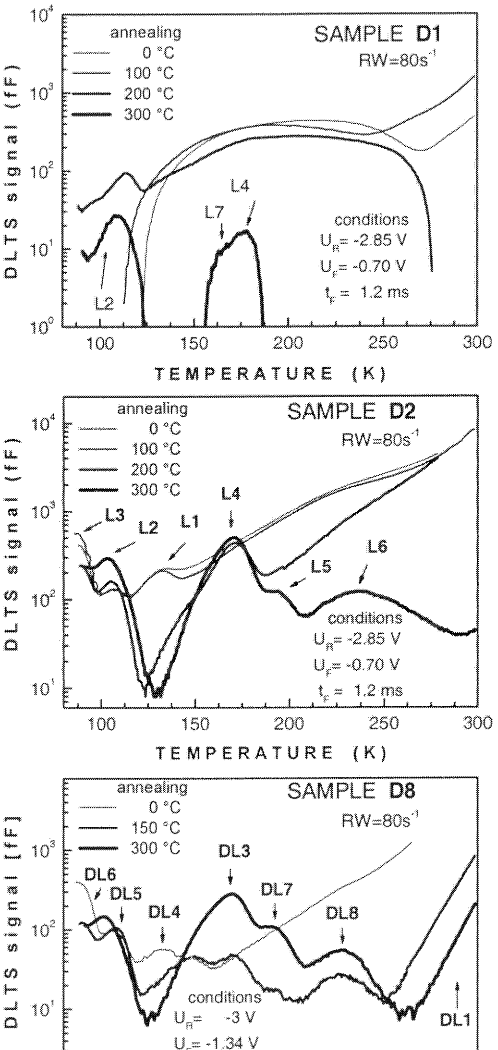

Fig. 7. Typical DLTS spectra measured on structures D1, D2 and D8 before and under isochronal annealing.

The values of the activation enthalpies ΔE_n of the detected electron deep levels L1-L7 and DL1-DL8 were extracted from an Arrhenius diagram (equation 6) and are listed in Tab.2.

4. Conclusion

Our results confirmed that the quality of MOS structure became much worse after the irradiation by high-energy Bi than Kr ions at the same fluency. The irradiation with a higher fluency had a harder negative influence on electrophysical properties of the structures. 14 identifiable radiation defects were created in irradiated structures. The annealing caused an improvement of structures properties, radiation induced defects in MOS structures were healed out considerably by annealing and so enabled to identify deep level parameters further.

Tab.2. Deep energy levels activation enthalpies ΔE_n and similar traps in literature.

Deep level	in sample		ΔE_n [meV]		Similar traps in literature
L1	D2		**224**		V^{-2}
L2	D2	D1	**156**	**170**	A-centre
L3	D2	D2	**121**	**154**	A-centre
L4	D1, D2		**305**		
L5	D1, D2		**334**		
L6	D2		**407**		V^{-2}
L7	D1		**196**		
DL1	D0, D6, D8		**611**		Au, 590meV,[17]
DL2	D6, D8		**523**		
DL3	D8	D6	**269**	**300**	V^{-2} [18]
DL4	D8		**246**		V^{-2} [18]
DL5	D8	D8	**171**	**141**	A-centre [17]
DL6	D8		**143**		A-centre [17]
DL7	D8		**360**		
DL8	D6, D8		**411**		
	Annealing [100, 200, 300°C]				

Acknowledgement

This work was supported by grant of the Slovak Grant Agency Vega, Project 1/0169/03.

REFERENCES

[1] SCRIVASTAVA, P.C. *et. al.* In: *Nuclear Inst. Methods Phys. Res. B 156*, 1999, pp. 105-109.
[2] NEUSTROEV, E.P *et. al.* In: *Nuclear Instr. and Methods Phys. Res. B 171*, 2000, pp. 443-447
[3] YARYKIN, N., CHO, C.R., ZUHR, R., ROZGONYI, G. In: *Physica B 273-274*, 1999, pp. 485-488
[4] STAŇO, J. SKURATOV, V. A., ŽIŠKA, M. In: *Solid State Phen.*, 82-84,2002, 453
[5] STUCHLÍKOVÁ, Ľ., HARMATHA, L., ŽIŠKA, M. In: Electronic Devices and Systems EDS'01. Brno, 2001, pp. 107-110.
[6] NEUSTROEV, E.P. *et. al.* In: *Nuclear Inst. Methods Phys. Res. B 146*, 1998, pp. 323-328
[7] BIERSACK, J. P., HAGGMARK, L. C.: In: *Nuclear Inst. Methods Phys. Res. B 174*, 1980, p. 257.
[8] www.elf.stuba.sk/semitest/
[9] PÍSEČNÝ, P., HARMATHA, L. In: APCOM 2002, Liptovský Mikuláš, Demänovská dolina : KF VA Liptovský Mikuláš, 2002, pp. 86-89, ISBN 80-8040-186-1
[10] SCHRODER, D. K. *Semiconductor Material and Device Characterization.* 2nd ed., Wiley, New York, 1998.
[11] NICOLLIAN, E. H., BREWS, J. R. *MOS (Metal Oxide Semiconductor) Physics and Technology.* Wiley, New York 1982.
[12] GURNIK, P., HARMATHA, L. *J. Electr. Eng.*, 48, 1-2, 1997, p.52.
[13] ZERBST, M. , ANGEW, Z.: *Physics*, 22, 1966, p.30.
[14] ŤAPAJNA, M., GURNIK, P., HARMATHA, L. In: *J. Electr. Eng.* 53, 2002, 9-10, 272.
[15] LANG, D.V.: *J. Appl. Phys. 45*, 1974, pp. 3014-3023
[16] PIERRET, R. F.: *Solid-St. Electronics*, 17, 1974, p.1257
[17] FUKUOKA, N., *et. al.* In:. *Appl. Phys.*, 32, 1993, no. 5A, pp. 2059-2062
[18] WATKINS, G.D. In: Deep Centers in Semiconductors (Si). Edited by S.T. Pantelides, Gordon and Breach Science Publishers, 1986, pp. 147-183